CHEMISTRY
A EUROPEAN JOURNAL

ChemPubSoc
Europe

DOI: 10.1002/chem.201200463

Nickel(II) and Copper(II) Complexes of β-Unsubstituted 5,15-Diazaporphyrins and Pyridazine-Fused Diazacorrinoids: Metal–Template Syntheses and Peripheral Functionalizations

Yoshihiro Matano,*[a] Tarou Shibano,[a] Haruyuki Nakano,[b] and Hiroshi Imahori[a, c, d]

Abstract: The present paper reports the first comprehensive study on the synthesis, structures, optical and electrochemical properties, and peripheral functionalizations of nickel(II) and copper(II) complexes of β-unsubstituted 5,15-diazaporphyrins (M-DAP; M = Ni, Cu) and pyridazine-fused diazacorrinoids (Ni-DACX; X = N, O). These two classes of compounds were constructed starting from mesityldipyrromethane by a metal–template method. Ni-DAP and Cu-DAP were prepared in high yields by the reaction of the respective metal–bis(dibromodipyrrin) complexes with NaN_3–CuX (X = I, Br), whereas Ni-DACN and Ni-DACO were formed as predominant products by the reaction with NaN_3. In both cases, the metal centers change their geometry from tetrahedral to square planar during the aza-annulation; X-ray crystallographic analyses of M-DAPs showed highly planar diazaporphyrin π planes. The Q band of Ni-DAP was redshifted and intensified compared with that of a nickel–porphyrin reference, due to the involvement of electronegative nitrogen atoms at the *meso* positions. It was found that the peripheral bromination of Ni-DAP and Ni-DACO occurred regioselectively to afford Ni-DAP-Br_4 and Ni-DACO-Br, respectively. These brominated derivatives underwent Stille reactions with tributyl(phenyl)stannane to give the corresponding phenylated derivatives, Ni-DAP-Ph_4 and Ni-DACO-Ph. On the basis of the absorption spectra and X-ray analysis, it has been concluded that the attached phenyl groups efficiently conjugate with the diazaporphyrin π system. The present results unambiguously corroborate that the β-unsubstituted DAPs and DACXs are promising platforms for the development of a new class of π-conjugated azaporphyrin-based materials.

Keywords: diazo compounds · macrocycles · porphyrinoids · template synthesis

Introduction

Recent developments of phthalocyanine-based functional dyes, pigments, and electronic materials have stimulated the search for a new azaporphyrin family that is easily accessible and finely tunable by conventional synthetic methods.[1] 5,15-Diazaporphyrin (DAP) is a structural hybrid of porphyrin and tetraazaporphyrin, and the frontier orbital characteristics of DAP reflect its D_{2h}-symmetric π system. The first synthesis of DAP by Fischer and co-workers dates back to 1936,[2] and since then, several types of β-substituted derivatives (2,3,7,8,12,13,17,18-octa-alkyl-DAP, tetrabenzo-DAP, and their relatives) have been reported.[3,4] The preceding studies have disclosed that the optical, electrochemical, and coordination properties of DAPs are distinguished from those of the two parent macrocycles. We envisioned that β-unsubstituted (β-free) DAP would also be a promising platform for the further development of azaporphyrin-based materials, because they are diversely tunable at the periphery. To our knowledge, however, very little information is available about β-free DAP derivatives,[5] and no attempt has been made to chemically functionalize their π systems. In this study, we aimed to establish practical methods for the synthesis and functionalization of β-free DAPs as well as to reveal the structure–property relationship of the resulting π systems. Herein, we report a highly efficient metal–template synthesis of nickel(II) and copper(II) complexes of β-free 5,15-diazaporphyrin (M-DAPs; M = Ni, Cu) and the unexpected formation of pyridazine-fused diazacorrinoids (Ni-DACX; X = N, O). The crystal structures, optical and electrochemical properties, and peripheral functionalizations of these two π systems are also reported.

[a] Prof. Dr. Y. Matano, T. Shibano, Prof. Dr. H. Imahori
Department of Molecular Engineering
Graduate School of Engineering, Kyoto University
Nishikyo-ku, Kyoto 615-8510 (Japan)
Fax: (+81) 75-383-2571
E-mail: matano@scl.kyoto-u.ac.jp

[b] Prof. Dr. H. Nakano
Department of Chemistry, Graduate School of Sciences
Kyushu University
Fukuoka 812-8581 (Japan)

[c] Prof. Dr. H. Imahori
Institute for Integrated Cell-Material Sciences (WPI-iCeMS)
Kyoto University
Nishikyo-ku, Kyoto 615-8510 (Japan)

[d] Prof. Dr. H. Imahori
Fukui Institute for Fundamental Chemistry
Kyoto University
Sakyo-ku, Kyoto 606-8103 (Japan)

Supporting information for this article is available on the WWW under http://dx.doi.org/10.1002/chem.201200463.

Results and Discussion

To achieve the first objective, namely the synthesis of M-DAPs, we applied a metal–template method by using dipyrrin–metal complexes and sodium azide (NaN_3), which had been employed for the synthesis of β-substituted DAP–copper complexes.[6] Scheme 1 and Table 1 summarize the present results.

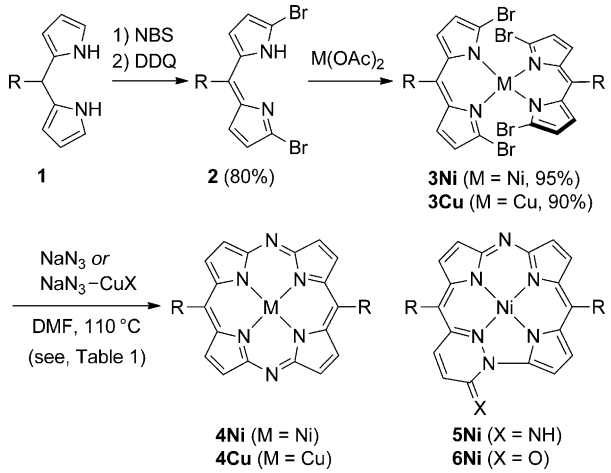

Scheme 1. Synthesis of **4Ni**, **4Cu**, **5Ni**, and **6Ni**. R = 2,4,6-$Me_3C_6H_2$.

Table 1. The metal–template aza-annulation of **3M** (**M**=**Ni**, **Cu**).[a]

Entry	3M	Reagents	Products (Yields [%])[b]
1	**3Ni**	NaN_3 (7 equiv)	**4Ni** (5), **5Ni** (13), **6Ni** (15)
2	**3Ni**	NaN_3 (4 equiv)	**4Ni** (12), **5Ni** (13), **6Ni** (20)
3	**3Ni**	NaN_3–CuI (8 equiv)	**4Ni** (86)
4	**3Ni**	NaN_3–CuI (4 equiv)	**4Ni** (88)
5	**3Ni**	NaN_3–CuBr (4 equiv)	**4Ni** (82)
6	**3Cu**	NaN_3–CuI (4 equiv)	**4Cu** (89)

[a] [**3M**] = 0.5–1.5 mM. [b] Isolated yields based on **3M**.

Consecutive treatment of mesityldipyrromethane **1** (mesityl = 2,4,6-$Me_3C_6H_2$) with *N*-bromosuccinimide (NBS) and 2,3-dichloro-5,6-dicyanobenzoquinone (DDQ) gave dibromodipyrrin **2** in 80% yield. Complexation between **2** and $Ni(OAc)_2$ proceeded smoothly to give bis(dibromodipyrrin)-nickel(II) complex **3Ni** in 95% yield. Compound **3Ni** was also obtained in 79% yield (based on **1**) without isolation of **2**. Heating a mixture of **3Ni**, NaN_3 (7 equiv), and DMF at 110 °C for a few hours afforded three major products, which were separable from one another by silica-gel column chromatography. The purple solid (R_f = 0.6; hexane/EtOAc 5:1) was an expected product, Ni-DAP (**4Ni**), whereas the green solids (R_f = 0.3 and 0.2) were found to be unexpected products, Ni-DACN (**5Ni**) and Ni-DACO (**6Ni**).[7] The structures of these products were determined on the basis of the spectral data, elemental analyses, and X-ray diffraction analyses (see below).[8] Compound **6Ni** was formed via hydrolysis of the imine moiety of **5Ni** during the reaction or column chromatography. In fact, **5Ni** was quantitatively transformed to **6Ni** by treatment with an aqueous HCl solution. The yields and the distribution of **4Ni**/**5Ni**/**6Ni** varied to some extent depending on the reaction conditions, although Ni-DACs (**5Ni**/**6Ni**) were always formed predominantly (Table 1, entries 1 and 2). To our surprise, however, the addition of copper(I) salts dramatically changed the reaction outcome. When NaN_3 was treated with CuI (8 equiv each) in DMF before the addition of **3Ni**, Ni-DAP **4Ni** was exclusively formed in 86% yield (Table 1, entry 3). It seemed that CuN_3 was generated as an active reagent from CuI and NaN_3.[9] The amounts of NaN_3–CuI could be reduced to 4 equiv without decreasing the yield of **4Ni** (Table 1, entry 4). The use of CuBr was also effective for the synthesis of **4Ni** (Table 1, entry 5). Under the NaN_3–CuI condition, **3Cu** was converted to **4Cu**[5] in 89% yield (Table 1, entry 6). The high-yield formation of **4M** (**M**=**Ni**, **Cu**; constantly >85%) in the NaN_3–CuI system was reproducible.[10] These results definitely show that the copper-assisted metal–template method is promising for the synthesis of β-free diazaporphyrin–nickel(II) and copper(II) complexes.[11]

The pyridazine-fused diazacorrinoid skeleton in **5Ni** and **6Ni** is unprecedented, and its formation is worth noting. Scheme 2 illustrates a plausible reaction pathway leading to

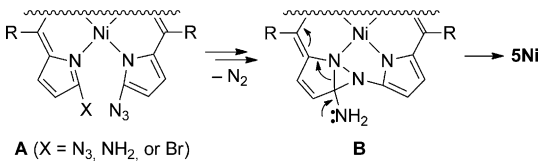

Scheme 2. A plausible reaction pathway for the formation of **5Ni** in the NaN_3 system. R = 2,4,6-$Me_3C_6H_2$.

5Ni. In the absence of CuI, the azido moiety in species **A** (X = N_3 or NH_2) may add to the N=C(α) bond of the adjacent pyrrole ring accompanied by evolution of N_2 to generate species **B** or its tautomer. The subsequent skeletal rearrangement of the diazabicyclo[3.1.0]hexene ring in **B** leads to **5Ni**. In the NaN_3–CuI system, the copper is likely to enhance the leaving ability of X (X = Br) in **A** through the coordination or oxidative addition, which results in the exclusive formation of **4Ni**. In both systems, the high affinity of nickel(II) to adopt a square-planar geometry plays a crucial role in promoting the aza-annulation steps.

The ^{1}H NMR spectrum of **4Ni** in CD_2Cl_2 showed two kinds of pyrrole-β protons at δ = 8.78 and 9.14 ppm (each, d, 4H), whereas the ^{1}H NMR spectra of **5Ni** and **6Ni** (Figure 1) displayed six kinds of pyrrole-β protons (each, 1H, d, J = 4.3–5.1 Hz) and two olefinic protons (each, d, 1H, J = 9.7–9.9 Hz). All the peripheral protons of **5Ni** and **6Ni** were assigned by ^{1}H–^{1}H COSY and NOESY techniques. In the IR spectrum of **6Ni** (KBr pellet), the C=O stretching vibration mode was detected at 1682 cm^{-1}. The structures of **3M**, **4M**, and **5Ni** were further elucidated by X-ray crystallography.[12] The ORTEP diagrams are shown in Figures 2, 3, 4, and 5 together with selected bond lengths and angles. As

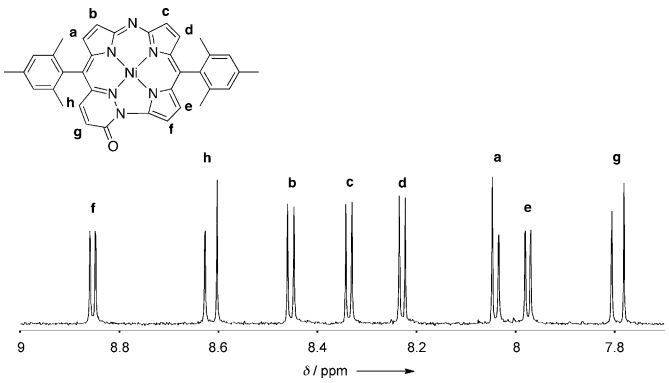

Figure 1. ^{1}H NMR spectrum (aromatic region) of **6Ni** in CD_2Cl_2.

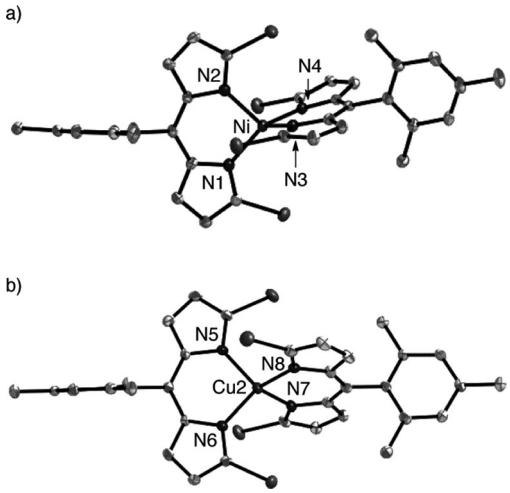

Figure 2. Crystal structures of a) **3Ni** and b) **3Cu** (30% probability ellipsoids). Hydrogen atoms are omitted for clarity. a) Selected bond lengths (Å) and angles (°): Ni–N1 1.950(4); Ni–N2 1.963(4); Ni–N3 1.973(3); Ni–N4 1.946(3); N1-Ni-N2 92.04(15); N1-Ni-N3 113.43(14); N1-Ni-N4 136.72(14); N2-Ni-N3 110.61(15); N2-Ni-N4 111.42(14); N3-Ni-N4 92.32(14). b) Selected bond lengths (Å) and angles (°) of one of the two independent molecules: Cu2–N5 1.954(4); Cu2–N6 1.948(4); Cu2–N7 1.964(4); Cu2–N8 1.946(4); N5-Cu2-N6 94.29(18); N5-Cu2-N7 129.02(18); N5-Cu2-N8 104.21(18); N6-Cu2-N7 104.18(17); N6-Cu2-N8 136.29(19); N7-Cu2-N8 94.34(18).

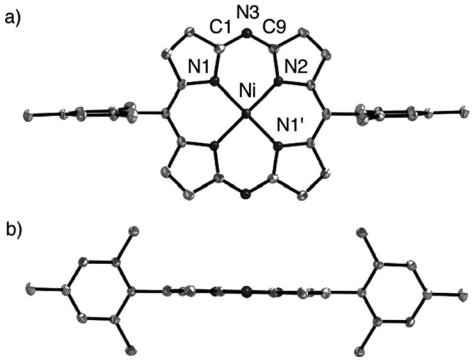

Figure 3. Crystal structure of **4Ni** (30% probability ellipsoids); hydrogen atoms are omitted for clarity. a) Top view and b) side view. Selected bond lengths (Å) and angles (°): Ni–N1 1.9145(16); Ni–N2 1.9131(16); N3–C1 1.325(3); N3–C9 1.321(3); N1-Ni-N2 89.33(7); N1′-Ni-N2 90.67(7); C1-N3-C9 120.14(18).

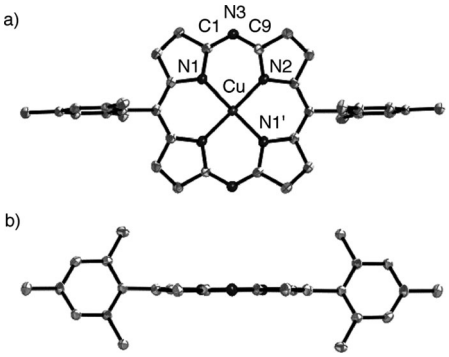

Figure 4. Crystal structure of **4Cu** (30% probability ellipsoids); hydrogen atoms are omitted for clarity. a) Top view and b) side view. Selected bond lengths (Å) and angles (°): Cu–N1 1.953(2); Cu–N2 1.945(3); N3–C1 1.321(4); N3–C9 1.329(4); N1-Cu-N2 89.42(10); N1′-Cu-N2 90.58(10); C1-N3-C9 122.2(3).

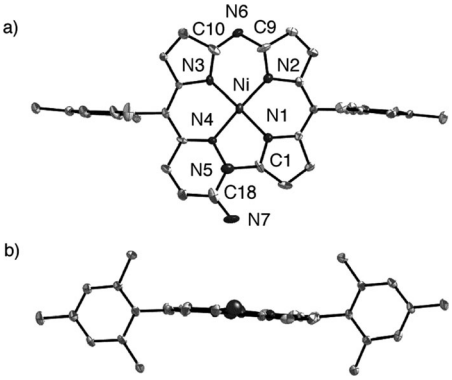

Figure 5. Crystal structure of **5Ni** (30% probability ellipsoids); hydrogen atoms are omitted for clarity. a) Top view and b) side view. Selected bond lengths (Å) and angles (°): Ni–N1 1.832(7); Ni–N2 1.855(7); Ni–N3 1.832(7); Ni–N4 1.875(6); N4–N5 1.414(10); N5–C1 1.438(11); N5–C18 1.357(14); N6–C9 1.357(10); N6–C10 1.294(11); N7–C18 1.314(14); N1-Ni-N2 92.1(3); N2-Ni-N3 90.3(3); N3-Ni-N4 93.2(3); N1-Ni-N4 84.4(3); N1-C1-N5 110.7(8); C1-N5-N4 114.5(7); C1-N5-C18 121.5(8); N5-C18-N7 115.9(9); C9-N6-C10 115.8(8).

shown in Figure 1a, the nickel center in **3Ni** adopts a distorted tetrahedral geometry with Ni–N bond lengths of 1.950(4)–1.973(3) Å and endocyclic N-Ni-N bond angles of 92.04(15)–92.32(14)°. The dihedral angle between two N-Ni-N planes of **3Ni** (83.6°) is considerably larger than that of α,α′-unsubstituted analogue (38.5°) reported by Scott and co-workers.[13] This is attributable to the electrostatic repulsion between the facing bromine atoms in **3Ni**. In sharp contrast, each nickel center in **4Ni** and **5Ni** adopts a square-planar geometry at the core (Figures 3 and 5). The DAP π plane of **4Ni** is highly planar (root mean square of deviations of the 24 atoms from the mean π plane (Δd_{RMS} = 0.018 Å) compared with the DAC π plane of **5Ni** (Δd_{RMS} = 0.042 Å; Figure S1 in the Supporting Information). The Ni–N distances of **4Ni** and **5Ni** are 1.913(2)–1.915(2) Å and 1.832(7)–1.875(6) Å, respectively, indicating that the N_4-coordination sphere differs slightly between these two macrocycles. The structures of **3Cu** and **4Cu** were also elucidated by X-ray crystallography (Figures 2b and 4).

The copper center in **3Cu** adopts a tetrahedral geometry with Cu–N bond lengths of 1.946(5)–1.964(5) Å, whereas that in **4Cu** adopts a square-planar geometry with Cu–N bond lengths of 1.945(3)–1.953(2) Å. It is evident that the aza-annulation from **3Cu** also produces a completely planar Cu–DAP π plane ($\Delta d_{RMS} = 0.019$ Å) in **4Cu**. The N(*meso*)–C(α) bond lengths of **4Ni** and **4Cu** are almost identical, whereas the C(α)-N(*meso*)-C(α) bond angle of **4Cu** is slightly wider than that of **4Ni**. This reflects the difference in the respective M–N bond lengths (1.953(2) and 1.945(3) Å for **4Cu**; 1.9145(16) and 1.9131(16) Å for **4Ni**).

To reveal the optical and electrochemical properties of the present β-free DAP and DAC π systems, UV/Vis absorption spectra and redox potentials of **4m**, **5Ni**, and **6Ni** as well as porphyrin reference **7** were recorded in CH_2Cl_2 (Table 2, Figure 6). In the absorption spectra of **4m**, Soret and Q bands appeared at $\lambda_{max} = 373$–397 and 571–577 nm, respectively. It should be noted that the Q band of **4Ni** is red-shifted and largely intensified compared with that of **7**. This is deeply related to the nondegenerate frontier orbitals of the DAP π systems[4d,e] (see below). The Ni-DAC derivatives **5Ni** and **6Ni** displayed broad and split absorption bands reaching $\lambda = 700$ nm due to their unsymmetrical structures.

Table 2. Optical and electrochemical data for **4**–**12**.[a]

	λ_{max} [nm] (log ε)	E_{redox} [V][b]
4Ni	373 (4.8), 390 (4.9), 571 (4.8)	+0.80, −1.40, −2.02
4Cu	384 (5.0), 397 (5.0), 577 (4.9)	+0.77, −1.37, −1.95
5Ni	406 (4.8), 556 (4.2), 592 (4.2), 638 (4.6)	N.m.
6Ni	386 (4.7), 580 (4.2), 623 (4.5)	+0.54, −1.56, −2.00
7	398 (5.4), 514 (4.2), 547 (3.9)	+1.00, +0.59, −1.77
8	401 (5.0), 587 (4.9)	N.m.
9	374 (4.9), 420 (5.1), 612 (4.8)	+0.68, −1.33, −2.01
10	385 (4.7), 589 (4.2), 626 (2.8)	N.m.
11	389 (4.7), 576 (4.2), 632 (4.4)	N.m.
12	389 (4.8), 591 (4.3), 635 (4.5)	+0.50, −1.54, −2.02

[a] Recorded in CH_2Cl_2; N.m. = not measured. [b] Redox potentials (vs. ferrocene/ferrocenium couple; with $Bu_4N^+PF_6^-$; Ag/Ag^+).

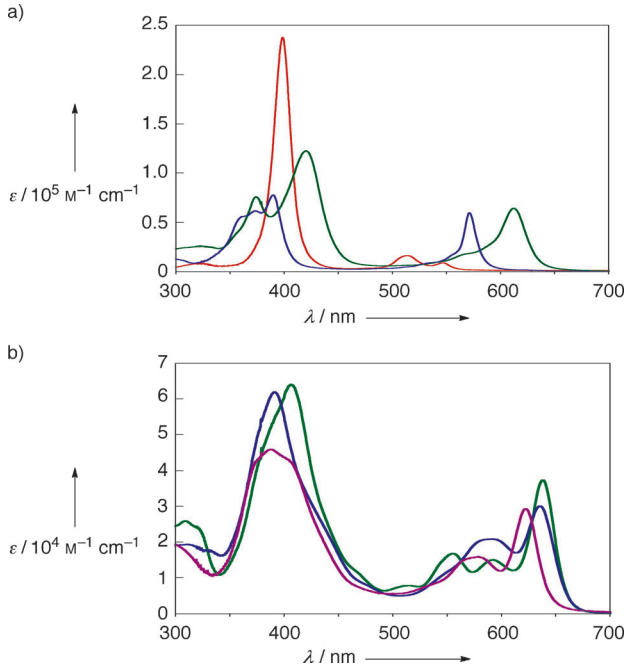

Figure 6. Absorption spectra of a) **4Ni** (blue), **7Ni** (red), **9** (green) and b) **5Ni** (green), **6Ni** (purple), **12** (blue) in CH_2Cl_2.

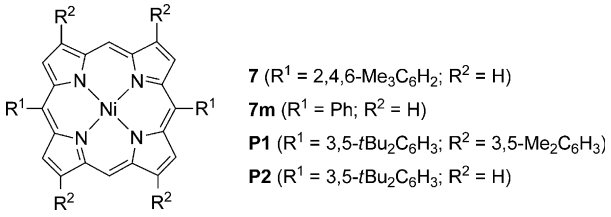

7 (R^1 = 2,4,6-$Me_3C_6H_2$; R^2 = H)
7m (R^1 = Ph; R^2 = H)
P1 (R^1 = 3,5-$tBu_2C_6H_3$; R^2 = 3,5-$Me_2C_6H_3$)
P2 (R^1 = 3,5-$tBu_2C_6H_3$; R^2 = H)

The incorporation of two nitrogen atoms into the *meso* positions induced anodic shifts for both oxidation and reduction potentials (E_{ox} and E_{red}) of the porphyrin π system; in cyclic voltammetry (CV) measurements, **4Ni** showed reversible redox processes at $E_{red,1} = -1.40$ and $E_{ox,1} = +0.80$ V, whereas **7** showed the respective processes at $E_{red,1} = -1.77$ and $E_{ox,1} = +0.59$ V vs. Fc/Fc^+ (Figure S2 in the Supporting Information). These results indicate that **4Ni** is harder to oxidize and easier to reduce than **7**. The Ni-DACO **6Ni** also showed reversible redox processes at $E_{red,1} = -1.56$ V and $E_{ox,1} = +0.54$ V. Accordingly, the energy gap (E_{ox}–E_{red}) decreases in the order: **7** (2.36 V) > **4Ni** (2.20 V) > **6Ni** (2.10 V), which correlates well with the order of the lowest excitation energies observed in their absorption spectra.

DFT calculations on the *meso*-phenyl-substituted models **4Nim** (R = Ph) and **7m** shed light on the character of their frontier orbitals (Figure 7). The replacement of two *meso* carbons by nitrogens (from **7m** to **4Nim**) breaks the near degeneracy of the frontier orbitals and stabilizes LUMO (from −2.31 to −2.89 eV) larger than HOMO (from −5.39 to −5.61 eV). As a result, the HOMO–LUMO gap of **4Nim** becomes narrow compared with that of **7m**. This is in good accordance with a trend of the redox potentials observed for the corresponding π systems, **4Ni** and **7**.

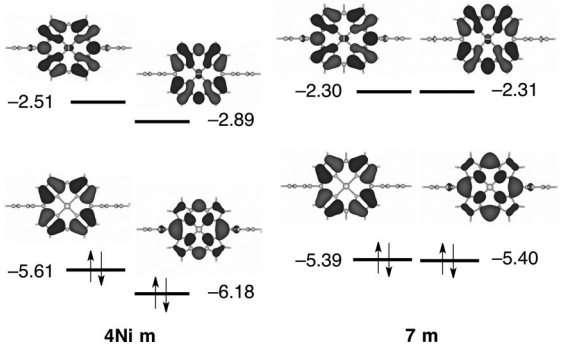

Figure 7. Molecular orbitals (HOMO−1, HOMO, LUMO, and LUMO+1) of **4Nim** and **7m**, and their energies (in eV) calculated by the B3LYP method.

Furthermore, we examined peripheral functionalizations of the β-free DAP and DAC π systems by using a bromination–cross-coupling strategy (Scheme 3). The Ni-DAP **4Ni**

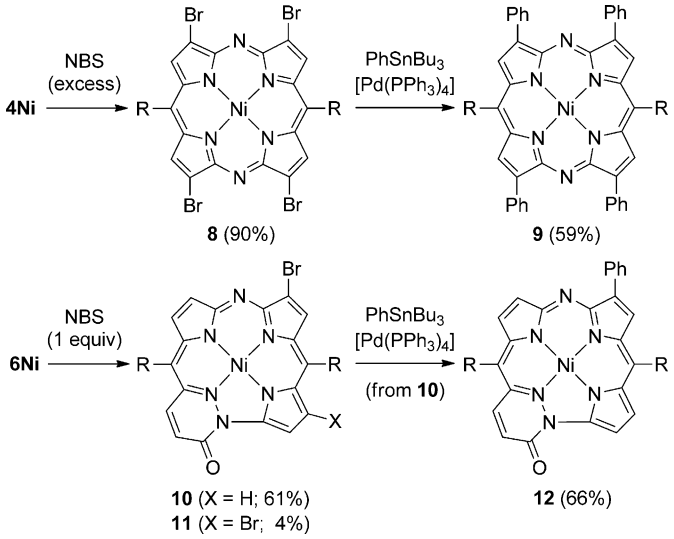

Scheme 3. Functionalizations of **4Ni** and **6Ni**. R = 2,4,6-$Me_3C_6H_2$.

reacted with excess NBS in $CHCl_3$ to give Ni-DAP-Br_4 **8** in 90% yield. It is of interest that the bromination of **4Ni** occurred regioselectively at the pyrrole-β carbons apart from the *meso*-mesityl groups, probably due to the steric reason. The Stille coupling of **8** with tributyl(phenyl)stannane proceeded smoothly in the presence of $[Pd(PPh_3)_4]$ catalyst to give Ni-DAP-Ph_4 **9**. According to a similar protocol, the Ni-DACO **6Ni** was also converted to DACO-Ph **12** via Ni-DACO-Br **10** (main product in bromination).

The crystal structures of **9** and Ni-DACO-Br_2 **11** (minor product in bromination) were elucidated by X-ray crystallography. As shown in Figures 8 and 9, compounds **9** and **11**

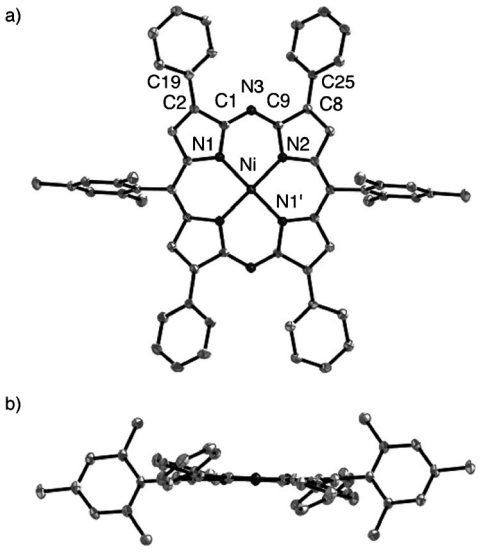

Figure 8. Crystal structure of **9** (30% probability ellipsoids); hydrogen atoms are omitted for clarity. a) Top view and b) side view. Selected bond lengths (Å) and angles (°): Ni–N1 1.923(2); Ni–N2 1.920(2); N3–C1 1.322(3); N3–C9 1.319(3); C2–C19 1.487(3); C8–C25 1.485(3); N1-Ni-N2 89.12(9); N1′-Ni-N2 90.88(9), C1-N3-C9 121.4(2); C1-C2-C19 128.6(2); C9-C8-C25 127.5(2).

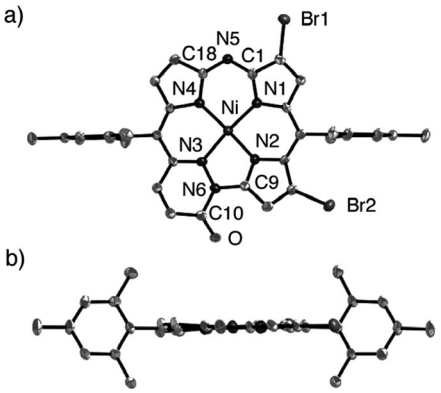

Figure 9. Crystal structure of **11** (30% probability ellipsoids); hydrogen atoms are omitted for clarity. a) Top view and b) side view. Selected bond lengths (Å) and angles (°): Ni–N1 1.857(5); Ni–N2 1.825(5); Ni–N3 1.898(5); Ni–N4 1.847(5); N3–N6 1.385(6); N5–C1 1.342(7); N5–C18 1.322(7); N6–C9 1.392(8); N6–C10 1.418(7); C10–O 1.217(7); N1-Ni-N2 90.7(2); N2-Ni-N3 83.2(2); N3-Ni-N4 93.6(2); N4-Ni-N1 92.5(2); N2-C9-N6 114.4(5); C9-N6-N3 112.7(5); C9-N6-C10 121.9(5); N6-C10-O 119.6(6); C1-N5-C18 119.6(5).

possess mostly planar π planes ($\Delta d_{RMS} = 0.045$ Å for **9**, 0.059 Å for **11**). It is noteworthy that dihedral angles between the β-phenyl rings and the mean DAP π plane in **9** (16.2–34.6°) are much narrower than those between the β-xylyl rings and the mean porphyrin π plane in nickel porphyrin **P1** (48.0–53.4°) reported by Osuka and co-workers.[12] This is attributable to the different steric effects of the *meso* bridges, nitrogen atom (in **9**) and CH (in **P1**); because **9** has no substituent on the *meso* nitrogen atoms, the β-phenyl rings can lean to the DAP π plane to a large extent.

In the absorption spectra, both Soret and Q bands of **9** are redshifted by $\lambda = 30$ and 41 nm, respectively, relative to the corresponding absorption bands of **4Ni** (Figure 6). The degree of β-substitution-induced redshifts observed for the NiDAP derivatives **9** versus **4Ni** is appreciably larger than that observed for the Ni-porphyrin counterparts **P1**[14] versus **P2**[15] with the same *meso*-aryl groups ($\Delta\lambda_{Soret} = 19$ nm; $\Delta\lambda_{Q} = 16$ nm). Obviously, the β-phenyl groups in **9** are conjugated with the porphyrin π system more efficiently than are the β-xylyl groups in **P1**, which agrees well with the results on the X-ray diffraction analyses. The effective π conjugation was also observed for **12**, which exhibited a redshift of 12 nm for the longest Q band relative to **6Ni** (Figure 6).

Conclusion

We successfully established an efficient metal–template synthesis of β-free 5,15-diazaporphyrin-nickel and -copper complexes by using the NaN_3–CuX reagents. In addition, we unexpectedly found that a new azaporphyrin family, the pyridazine-fused diazacorrinoides, was produced predominantly under the classical condition (NaN_3/DMF). Furthermore, we demonstrated for the first time that the successive bromination–Stille coupling reactions could be utilized for the regio-

selective functionalizations of the DAP and DAC π systems at the periphery. The newly constructed diazaporphyrin derivatives exhibited the characteristic properties owing to the electronic and steric effects of the *meso* nitrogen atoms. The present results unambiguously corroborate that the β-free DAPs and DACs are promising platforms for the development of a new class of π-conjugated azaporphyrin-based materials.

Experimental Section

All melting points were recorded on a Yanagimoto micromelting point apparatus and are uncorrected. ^{1}H and ^{13}C{^{1}H} NMR spectra were recorded on a JEOL EX400, AL300, or ECA-600P spectrometers. Chemical shifts are reported in ppm as the relative values versus tetramethylsilane. Selected ^{1}H NMR spectra are shown in Figures S3–S12 in the Supporting Information. ^{1}H–^{1}H COSY and NOESY spectra were recorded on JEOL ECA-600P and JEOL ECS-400 spectrometers, respectively. HRMS were obtained on a Thermo EXACTIVE spectrometer. IR spectra were obtained on a JASCO FT/IR-470 Plus spectrometer. UV/Vis absorption spectra were obtained on a PerkinElmer Lambda 900 UV/Vis/NIR spectrometer. Electrochemical measurements were performed on a CH Instruments model 660 A electrochemical workstation by using a glassy carbon working electrode, a platinum wire counter electrode, and an Ag/Ag$^+$ [0.01 M $AgNO_3$, 0.1 M nBu$_4$NPF$_6$ (MeCN)] reference electrode. The potentials were calibrated with ferrocene/ferrocenium [E_{mid} = +0.20 V vs Ag/$AgNO_3$]. Elemental analyses were performed at the Microanalytical Laboratory of Kyoto University. Mesityldipyrromethane **1** was prepared according to the reported procedure.[16] Sodium azide (>98%), copper iodide (>99.5%), copper bromide (>95%), and dehydrated DMF (water content <0.005%) were purchased from Wako Pure Chemical Industries. All chemicals and solvents were of reagent-grade quality and used without further purification. TLC was performed with Alt. 5554 DC-Alufolien Kieselgel 60 F254 (Merck), and preparative column chromatography was performed by using UltraPure SilicaGel (230–400 mesh; SiliCycle Inc.) or silica gel 60 (spherical, neutrality; Nacalai tesque). All the reactions were performed under an argon atmosphere.

Synthesis of 2: Compound **1** (3.0 g, 11 mmol) was taken in dry THF (150 mL) and cooled to −78 °C. NBS (4.0 g, 22 mmol) was added in two portions over 1 h. After NBS dissolved completely, a THF solution (15 mL) of DDQ (2.60 g, 11.4 mmol) was added dropwise over 10 min. The reaction mixture was warmed to RT and then evaporated under reduced pressure to give a solid residue, which was washed with hexane/CH_2Cl_2. The residue was then immediately subjected to silica-gel column chromatography (hexane as an eluent) to give **2** (R_f = 0.7) as a yellow solid (3.8 g, 80%). M.p. 137 °C; ^{1}H NMR (400 MHz, CD_2Cl_2): δ = 2.05 (s, 6H; *ortho*-Me), 2.33 (s, 3H; *para*-Me), 6.26 (d, J = 4.4 Hz, 2H; pyrrole-β), 6.29 (d, J = 4.4 Hz, 2H; pyrrole-β), 6.92 ppm (s, 2H; ArH); ^{13}C{^{1}H} NMR (CD_2Cl_2): δ = 140.6, 138.6, 137.1, 129.1, 128.3, 120.9, 21.2, 19.9 ppm; HRMS (ESI): *m/z* calcd for $C_{18}H_{17}N_2Br_2$: 418.9758 [M+H]$^+$ (^{78}Br,^{78}Br); found: 418.9753; UV/Vis (CH_2Cl_2): λ_{max} (ε) = 445 nm (21000 M^{-1}cm^{-1}); elemental analysis calcd (%) for $C_{18}H_{16}Br_2N_2$ (M_w): C 51.46, H 3.84, N 6.67, Br 38.01; found: C 51.47, H 3.70, N 6.57, Br 38.11.

Synthesis of 3Ni: To a solution of **2** (2.0 g, 4.8 mmol) in CH_2Cl_2 (45 mL) and MeOH (30 mL) was added Ni(OAc)$_2$·4H$_2$O (0.59 g, 2.4 mmol). After 1 h of stirring at RT, the mixture was evaporated under reduced pressure, and a solid residue was recrystallized from MeOH/CH_2Cl_2 to give **3Ni** as a green solid (2.03 g, 95%). Compound **3Ni** could be prepared in 79% yield (based on **1**) without isolating **2**. M.p. >300 °C; HRMS (ESI): *m/z* calcd for $C_{36}H_{31}Br_4N_4Ni$: 892.8636 [M+H]$^+$; found: 892.8619; UV/Vis (CH_2Cl_2): λ_{max} (ε) = 352 (20000), 447 (34000), 518 nm (81000 M^{-1}cm^{-1}); elemental analysis calcd (%) for $C_{36}H_{30}Br_4N_4Ni$ (M_w): C 48.21, H 3.37, N 6.25, Br 35.63; found: C 47.95, H 3.09, N 6.26, Br 35.54.

Synthesis of 3Cu: To a solution of **2** (35.4 mg, 0.0843 mmol) in MeOH (20 mL) was added Cu(OAc)$_2$ (7.2 mg, 0.040 mmol). After 1 h of stirring at RT, the mixture was evaporated under reduced pressure, and a solid residue was recrystallized from CH_2Cl_2/MeOH to give **3Cu** as a green solid (34.3 mg, 90%). M.p. >300 °C; HRMS (ESI): *m/z* calcd for $C_{36}H_{31}Br_4CuN_4$: 897.8573 [M+H]$^+$; found: 897.8567; UV/Vis (CH_2Cl_2): λ_{max} (ε) = 462 (35000), 515 nm (48000 M^{-1}cm^{-1}); elemental analysis calcd (%) for $C_{36}H_{30}Br_4CuN_4$ (M_w): C 47.95, H 3.35, N 6.21, Br 35.44; found: C 47.72, H 3.33, N 6.08, Br 35.34.

Reaction of 3Ni with NaN_3 (typical procedure): A mixture of **3Ni** (500 mg, 0.557 mmol), sodium azide (157 mg, 2.42 mmol), and DMF (500 mL) was stirred at 110 °C. After 1 h, toluene and brine were added, and the organic phase was washed with brine several times. The toluene layer was separated, washed with water twice, and evaporated under reduced pressure to leave a solid residue, which was then subjected on silica-gel column chromatography (hexane/EtOAc 5:1). The major three products, **4Ni** (R_f = 0.6; 39.9 mg, 12%), **5Ni** (R_f = 0.3; 43.4 mg, 13%), and **6Ni** (R_f = 0.2; 68.1 mg, 20%) were isolated separately. The yields and the distribution of **4Ni/5Ni/6Ni** varied to some extent depending on the reaction conditions employed. **4Ni**: m.p. >300 °C; ^{1}H NMR (400 MHz, CD_2Cl_2): δ = 1.79 (s, 12H; *para*-Me), 2.61 (s, 6H; *ortho*-Me), 7.29 (s, 4H; Ar-*meta*), 8.78 (d, J = 4.8 Hz, 4H; pyrrole-β), 9.14 ppm (d, J = 4.8 Hz, 4H; pyrrole-*b*); ^{13}C{^{1}H} NMR (100 MHz, CD_2Cl_2): δ = 151.0, 144.5, 139.3, 139.0, 135.5, 134.5, 133.8, 128.3, 121.2, 30.1, 21.5 ppm; HRMS (ESI): *m/z* calcd for $C_{36}H_{30}N_6Ni$: 604.1885 [M]$^+$; found: 604.1847; UV/Vis (CH_2Cl_2): λ_{max} (ε) = 373 (62000), 390 (78000), 571 nm (60000 M^{-1}cm^{-1}); elemental analysis calcd (%) for $C_{36}H_{30}N_6Ni$ (M_w): C 71.43, H 5.00, N, 13.88; found: C 69.76, H 5.07, N 13.09. **5Ni**: m.p. >300 °C; ^{1}H NMR (400 MHz, $CDCl_3$): δ = 1.82 (s, 6H; *ortho*-Me), 1.91 (s, 6H; *ortho*-Me), 2.53 (s, 3H; *para*-Me), 2.54 (s, 3H; *para*-Me), 7.18 (s, 4H; Ar-*meta*), 7.43 (d, J = 9.8 Hz, 1H; vinyl), 7.91 (d, J = 9.8 Hz, 1H; vinyl), 7.99 (d, J = 5.0 Hz, 1H; pyrrole-β), 8.02 (d, J = 4.4 Hz, 1H; pyrrole-β), 8.24 (d, J = 4.8 Hz, 1H; pyrrole-β), 8.27 (br-s, 1H; NH), 8.40 (d, J = 4.8 Hz, 1H; pyrrole-β), 8.49 (d, J = 5.0 Hz, 1H; pyrrole-β), 9.06 ppm (br-s, 1H; pyrrole-β); ^{1}H NMR (400 MHz, CD_2Cl_2): δ = 1.82 (s, 6H; *ortho*-Me), 1.91 (s, 6H; *ortho*-Me), 2.53 (s, 3H; *para*-Me), 2.54 (s, 3H; *para*-Me), 7.20 (s, 4H; Ar-*meta*), 7.46 (d, J = 9.7 Hz, 1H; vinyl), 7.88 (d, J = 9.7 Hz, 1H; vinyl), 7.99 (2×d, J = 4.8 Hz, each 1H; pyrrole-β), 8.20 (d, J = 4.4 Hz, 1H; pyrrole-β), 8.34 (d, J = 4.8 Hz, 1H; pyrrole-β), 8.34 (s, 1H; NH), 8.44 (d, J = 4.8 Hz, 1H; pyrrole-β), 9.06 ppm (d, J = 4.8 Hz, 1H; pyrrole-β); HRMS (ESI): *m/z* calcd for $C_{36}H_{32}N_7Ni$: 620.2067 [M+H]$^+$; found: 620.2061; UV/Vis (CH_2Cl_2): λ_{max} (ε) = 406 (64000), 556 (17000), 592 (15000), 638 nm (37000 M^{-1}cm^{-1}); IR (KBr): $\tilde{\nu}_{max}$ = 3303 (NH) cm^{-1}; elemental analysis calcd (%) for $C_{36}H_{31}N_7Ni$ (M_w): C 69.70, H 5.04, N 15.80; found: C 69.26, H 5.19, N 15.70%. **6Ni**: m.p. >300 °C; ^{1}H NMR (400 MHz, CD_2Cl_2): δ = 1.82 (s, 6H; *ortho*-Me), 1.92 (s, 6H; *ortho*-Me), 2.55 (s, 3H; *para*-Me), 2.56 (s, 3H; *para*-Me), 7.19 (s, 2H; Ar-*meta*), 7.22 (s, 2H; Ar-*meta*), 7.83 (d, J = 9.9 Hz, 1H; vinyl), 8.02 (d, J = 4.4 Hz, 1H; pyrrole-β), 8.05 (d, J = 5.1 Hz, 1H; pyrrole-β), 8.26 (d, J = 4.8 Hz, 1H; pyrrole-β), 8.39 (d, J = 4.8 Hz, 1H; pyrrole-β), 8.50 (d, J = 5.1 Hz, 1H; pyrrole-β), 8.63 (d, J = 9.9 Hz, 1H; vinyl), 8.91 ppm (d, J = 4.4 Hz, 1H; pyrrole-β); HRMS (ESI): *m/z* calcd for $C_{36}H_{31}N_6NiO$: 621.1907 [M+H]$^+$; found: 621.1899; UV/Vis (CH_2Cl_2): λ_{max} (ε) = 386 (46000), 580 (16000), 623 nm (29000 M^{-1}cm^{-1}); IR (KBr): $\tilde{\nu}_{max}$ = 1682 cm^{-1} (C=O).

Reaction of 3Ni with NaN_3–CuI: A mixture of CuI (501 mg, 2.64 mmol), sodium azide (171 mg, 2.63 mmol), and DMF (200 mL) was stirred at RT for 10 min, during which the color of the solution changed to black. Compound **3Ni** (300 mg, 0.334 mmol) was then added in one portion, and the resulting mixture was heated to 110 °C. After 1 h, toluene and brine were added, and the organic phase was washed with water several times. The organic phase was dried over Na_2SO_4 and evaporated under reduced pressure to leave a solid residue, which was then subjected on silica-gel column chromatography (hexane/EtOAc 5:1) followed by reprecipitation from CH_2Cl_2/MeOH. The major product, **4Ni** was obtained as a purple solid (173 mg, 86%). In this reaction, **5Ni** and **6Ni** were not produced in detectable amounts. When 4 equiv of NaN_3 and CuI were used, **4Ni** was obtained in 88% yield. If CuBr was used instead of CuI, **4Ni** was isolated in 82% yield.

Reaction of 3Cu with NaN_3–CuI: A mixture of CuI (95 mg, 0.50 mmol), sodium azide (33 mg, 0.51 mmol), and DMF (300 mL) was stirred at RT for 1 h. Compound **3Cu** (100 mg, 0.111 mmol) was then added in one portion, and the resulting mixture was heated to 110 °C. After 1 h, toluene and brine were added, and the organic phase was washed with brine several times. The organic phase was dried over Na_2SO_4 and evaporated under reduced pressure to leave a solid residue, which was then subjected on silica-gel column chromatography (hexane/ethyl acetate 5:1) followed by reprecipitation from CH_2Cl_2/MeOH. The major product, **4Cu** (R_f = 0.5) was obtained as a purple solid (60.3 mg, 89 %). M.p. >300 °C; HRMS (ESI): *m/z* calcd for $C_{36}H_{31}CuN_6$: 610.1901 $[M+H]^+$; found: 610.1888; UV/Vis (CH_2Cl_2): λ_{max} (ε) = 384 (95000), 397 (93000), 577 nm (88000 $M^{-1}cm^{-1}$). Although this compound was described in a patent,[5] the yield and the spectral data were not reported.

Synthesis of 7: A mixture of 5,15-dimesitylporphyrin (30 mg, 0.055 mmol), $NiCl_2$ (7.7 mg, 0.059 mmol), and DMF (5 mL) was stirred at 100 °C for 10 h. After cooling to RT, CH_2Cl_2 was added, and the resulting solution was washed with an aqueous $NaHCO_3$ solution and brine, dried over Na_2SO_4, and evaporated under reduced pressure. The solid residue was then subjected on silica-gel column chromatography (CH_2Cl_2/hexane 1:1). Compound **7** (R_f = 0.8) was isolated as a purple solid (18.9 mg, 57 %). M.p. >300 °C; ^{1}H NMR (400 MHz, CD_2Cl_2): δ = 1.77 (s, 12H; *para*-Me), 2.60 (s, 6H; *ortho*-Me), 7.27 (s, 4H; Ar-H), 8.76 (d, J = 4.9 Hz, 4H; pyrrole-β), 9.18 (d, J = 4.9 Hz, 4H; pyrrole-β), 9.94 ppm (s, 2H; *meso*-H); ^{13}C{^{1}H} NMR (100 MHz, CD_2Cl_2): δ = 21.46, 21.56, 105.12, 117.17, 128.18, 131.59, 132.83, 137.60, 138.35, 139.38, 143.16 ppm; HRMS (ESI): *m/z* calcd for $C_{38}H_{33}N_4Ni$: 603.2059 $[M+H]^+$; found: 603.2054; UV/Vis (CH_2Cl_2): λ_{max} (ε) = 398 (230000), 514 (16000), 547 nm (8800 $M^{-1}cm^{-1}$).

Synthesis of 8: To a solution of **4Ni** (44 mg, 0.073 mmol) in $CHCl_3$ (10 mL) was added NBS (174 mg, 0.98 mmol), and the resulting mixture was heated at reflux. After 10 h, the solvent was removed under reduced pressure, and a solid residue was purified by column chromatography on silica gel (CH_2Cl_2/hexane 1:1 as eluents) to give **8** (R_f = 0.8) as a purple solid (60 mg, 90 %). M.p. >300 °C; ^{1}H NMR (400 MHz, CD_2Cl_2): δ = 1.79 (s, 12H; *para*-Me), 2.60 (s, 6H; *ortho*-Me), 7.29 (s, 4H; Ar-H), 8.82 ppm (s, 4H; pyrrole-β); HRMS (ESI): *m/z* calcd for $C_{36}H_{27}Br_4N_6Ni$: 916.8384 $[M+H]^+$; found: 916.8361; UV/Vis (CH_2Cl_2): λ_{max} (ε) = 364 (61000), 401 (97000), 587 nm (77000 $M^{-1}cm^{-1}$).

Synthesis of 9: A mixture of **8** (20.1 mg, 0.0218 mmol), tributyl(phenyl)stannane (64.8 mg, 0.176 mmol), $[Pd(PPh_3)_4]$ (2.3 mg, 0.0020 mmol), and DMF (5 mL) was stirred at 120 °C. After 3 h, toluene and water were added. The toluene layer was separated, washed with water, and evaporated under reduced pressure to leave a solid residue, which was then subjected on silica-gel column chromatography (hexane/CH_2Cl_2 4:1). Compound **9** (R_f = 0.7) was isolated as a green solid (11.8 mg, 59 %) after recrystallization from CH_2Cl_2–MeOH. M.p. >300 °C; ^{1}H NMR (400 MHz, CD_2Cl_2): δ = 1.90 (s, 12H; *para*-Me), 2.64 (s, 6H; *ortho*-Me), 7.33 (s, 4H; Ar-H), 7.56 (t, J = 7.3 Hz, 4H; Ph-*para*), 7.66 (t, J = 7.3 Hz, 8H; Ph-*meta*), 8.75 (d, J = 7.3 Hz, 8H; Ph-*ortho*), 8.88 ppm (s, 4H; pyrrole-β); ^{13}C{^{1}H} NMR (100 MHz, CD_2Cl_2): δ = 160.2, 154.9, 152.6, 147.1, 146.0, 133.3, 132.0, 131.2, 129.9, 129.0, 128.3, 121.2, 120.4, 30.1, 21.5 ppm; HRMS (ESI): *m/z* calcd for $C_{60}H_{47}N_6Ni$: 909.3210 $[M+H]^+$; found: 909.3205; UV/Vis (CH_2Cl_2): λ_{max} (ε) = 374 (70000), 420 (120000), 612 nm (64000 $M^{-1}cm^{-1}$).

Syntheses of 10 and 11: To a solution of **6Ni** (56.3 mg, 0.0905 mmol) in $CHCl_3$ (10 mL) was added NBS (16.2 mg, 0.0910 mmol), and the resulting mixture was stirred at RT. After 2 h, the solvent was removed under reduced pressure, and a solid residue was purified by column chromatography on silica gel (hexane/EtOAc 5:1) to give three major compounds, **11** (R_f = 0.6; 2.5 mg, 4 %), **10** (R_f = 0.5; 38.8 mg, 61 %), and **6Ni** (R_f = 0.3; 7.0 mg, 12 %). These compounds are separable, and their structures were characterized on the basis of NMR spectroscopy and MS. **10**: m.p. >300 °C; ^{1}H NMR (600 MHz, CD_2Cl_2): δ = 1.83 (s, 6H, *ortho*-Me), 1.91 (s, 6H, *ortho*-Me), 2.54 (s, 3H, *para*-Me), 2.55(s, 3H, *para*-Me), 7.21 (s, 2H, Ar-*meta*), 7.24 (s, 2H, Ar-*meta*), 7.80 (d, J = 9.9 Hz, 1H; vinyl), 8.00 (d, J = 4.4 Hz, 1H pyrrole-β), 8.06 (d, J = 4.9 Hz, 1H, pyrrole-β), 8.29 (s, 1H, pyrrole-β), 8.53 (d, J = 4.9 Hz, 1H, pyrrole-β), 8.62 (d, J = 9.9 Hz, 1H; vinyl), 8.85 ppm (d, J = 4.4 Hz, 1H, pyrrole-β); HRMS (ESI): *m/z* calcd for $C_{36}H_{30}BrN_6NiO$: 699.1012 $[M+H]^+$; found: 699.0982; UV/Vis (CH_2Cl_2): λ_{max} (ε) = 385 (45000), 589 (17000), 626 nm (26000 $M^{-1}cm^{-1}$); IR (KBr): $\tilde{\nu}_{max}$ = 1690 cm^{-1} (C=O). **11**: m.p. >300 °C; ^{1}H NMR (600 MHz, CD_2Cl_2): δ = 1.83 (s, 6H, *ortho*-Me), 1.86 (s, 6H, *ortho*-Me), 2.54 (s, 3H, *para*-Me), 2.55(s, 3H, *para*-Me), 7.19 (s, 2H, Ar-*meta*), 7.23 (s, 2H, Ar-*meta*), 7.79 (d, J = 9.9 Hz, 1H, vinyl), 8.04 (d, J = 5.4 Hz, 1H, pyrrole-β), 8.21 (s, 1H, pyrrole-β), 8.50 (d, J = 5.4 Hz, 1H, pyrrole-β), 8.58 (d, J = 9.9 Hz, 1H, vinyl), 8.95 ppm (s, 1H, pyrrole-β); HRMS (ESI): *m/z* calcd for $C_{36}H_{29}Br_2N_6NiO$: 777.0118 $[M+H]^+$; found: 777.0087; UV/Vis (CH_2Cl_2): λ_{max} (ε) = 389 (49000), 576 (17000), 632 nm (27000 $M^{-1}cm^{-1}$); IR (KBr): $\tilde{\nu}_{max}$ = 1690 cm^{-1} (C=O).

Synthesis of 12: A mixture **10** (38 mg, 0.054 mmol), tributyl(phenyl)stannane (22 mg, 0.060 mmol), $[Pd(PPh_3)_4]$ (6 mg, 0.005 mmol), and DMF (40 mL) was stirred at 120 °C. After 1 h, toluene and water were added. The toluene layer was separated, washed with water, and evaporated under reduced pressure to leave a solid residue, which was then subjected on silica-gel column chromatography (hexane/EtOAc 5:1). Compound **12** (R_f = 0.5) was isolated as a green solid (25 mg, 66 %) after recrystallization from CH_2Cl_2/MeOH. M.p. >300 °C; ^{1}H NMR (400 MHz, CD_2Cl_2): δ = 1.84 (s, 6H, *ortho*-Me), 1.95 (s, 6H, *ortho*-Me), 2.55 (s, 6H, *para*-Me), 7.24 (s, 2H, Ar-*meta*), 7.23 (s, 2H, Ar-*meta*), 7.45 (t, J = 7.7 Hz, 1H, Ph-*para*), 7.60 (dd, J = 7.7, 7.1 Hz, 2H, Ph-*meta*),7.80 (d, J = 9.8 Hz, 1H, vinyl), 7.98 (d, J = 4.3 Hz, 1H, pyrrole-β), 8.06 (d, J = 4.9 Hz, 1H, pyrrole-β), 8.38 (s, 1H, pyrrole-β), 8.53 (d, J = 4.9 Hz, 1H, pyrrole-β), 8.56 (d, J = 7.1 Hz, 2H, Ph-*ortho*), 8.63 (d, J = 9.8 Hz, 1H, vinyl), 8.87 ppm (d, J = 4.3 Hz, 1H, pyrrole-β); HRMS (ESI): *m/z* calcd for $C_{42}H_{35}N_6NiO$: 697.2220 $[M+H]^+$; found: 697.2218; UV/Vis (CH_2Cl_2): λ_{max} (ε) = 389 (62000), 591 (21000), 635 nm (30000 $M^{-1}cm^{-1}$); IR (KBr): $\tilde{\nu}_{max}$ = 1691 cm^{-1} (C=O).

X-ray crystallographic analyses: Single crystals of **3Ni**, **3Cu**, **4Ni**, **4Cu**, **5Ni**, **9**, and **11** were grown from CH_2Cl_2/MeOH at RT. X-ray crystallographic measurements were made on a Rigaku Saturn CCD area detector with graphite monochromated $Mo_{K\alpha}$ radiation (0.71070 Å) at −130 °C. The data were corrected for Lorentz and polarization effects. The structures were solved by using a direct method[17] and refined by full-matrix least squares techniques against F^2 by using SHELXL-97.[18] The nonhydrogen atoms were refined anisotropically, and hydrogen atoms were refined by using the rigid model. All calculations were performed by using CrystalStructure crystallographic software package,[19] except for the refinement. CCDC-860204 (**3Ni**), CCDC-860205 (**3Cu**), CCDC-860206 (**4Ni**), CCDC-860207 (**4Cu**), CCDC-861350 (**5Ni**), CCDC-860209 (**9**), and CCDC-860208 (**11**) contain the supplementary crystallographic data for this paper. These data can be obtained free of charge from The Cambridge Crystallographic Data Centre via www.ccdc.cam.ac.uk/data_request/cif.

Computational details: The structures of model compounds **4Nim** and **7m** were optimized by using DFT. The basis sets used were 6–311G(d,p) basis set[20] for H, C, and N and the Wachters–Hay all-electron basis set[21] supplemented with one f-function (exponent: 1.29) for Ni. The functional of DFT was Becke, three parameter, Lee–Yang–Parr (B3LYP) exchange–correlation functional.[22] We confirmed that the optimized geometries were not in saddle, but in stable points. As a result, the stable geometries of **4Nim** and **7m** became D_{2h} symmetry; in the optimized structures of model compounds, the *meso*-phenyl groups are perpendicular to the (diaza)porphyrin π planes. The Cartesian coordinates are summarized in Table S1 in the Supporting Information. All the calculations were carried out by using the Gaussian 09 suite of programs.[23] Selected molecular orbitals and their energies are summarized in Figure 7.

Acknowledgements

We thank Dr. Takashi Matsumoto (Rigaku corporation), Dr. Keiko Kuwata, and Dr. Haruo Fujita (Kyoto University) for the measurements of X-ray diffraction analysis of **5Ni**, HRMS, and 2D-NMR spectra, respectively. We also thank Prof. Hiroshi Shinokubo (Nagoya University) and Prof. Shigeki Kawabata (Toyama Prefectural University) for fruitful

discussion. This work was supported by Grants-in-Aid (π Space, Nos. 21108511 and 23108708) from MEXT, Japan.

[1] For example, see: a) *Phthalocyanines, Properties and Applications, Vol. I–IV* (Eds.: C. C. Leznoff, A. B. P. Lever), Wiley, New York, **1989**, **1993**, **1993**, **1996**; b) N. B. McKeown, *Phthalocyanine Materials: Synthesis, Structure and Function*, Cambridge University Press, Cambridge, **1998**; c) N. Kobayashi in *The Porphyrin Handbook, Vol. 2*, (Eds.: K. Kadish, R. M. Smith, R. Guilard), Academic Press, San Diego, **2000**, pp. 301–360; d) G. de La Torre, M. Nicolau, T. Torres in *Supramolecular Photosensitive and Electroactive Materials* (Ed.: H. S. Nalwa) Academic Press, San Diego, **2001**, pp. 1–111; e) M. S. Rodríguez-Morgade, G. de La Torre, T. Torres in *The Porphyrin Handbook, Vol. 15* (Eds.: K. Kadish, R. M. Smith, R. Guilard), Academic Press, San Diego, **2003**, pp. 125–159; f) K. Ishii, N. Kobayashi in *The Porphyrin Handbook, Vol. 16*, (Eds.: K. Kadish, R. M. Smith, R. Guilard), Academic Press, San Diego, **2003**, pp. 1–42; g) J. Mack, M. J. Stillman in *The Porphyrin Handbook, Vol. 16*, (Eds.: K. Kadish, R. M. Smith, R. Guilard), Academic Press, San Diego, **2003**, pp. 43–116.

[2] H. Fischer, H. Harberland, A. Müller, *Justus Liebigs Ann. Chem.* **1936**, *521*, 122.

[3] P. A. Stuzhin, O. G. Khelevina, *Coord. Chem. Rev.* **1996**, *147*, 41.

[4] For recent examples, see: a) S. Neya, H. Hori, K. Imai, Y. Kawamura-Konishi, H. Suzuki, Y. Shiro, T. Iizuka, N. Funasaki, *J. Biochem.* **1997**, *121*, 654; b) P. A. Stuzhin, M. Goeldner, H. Homborg, A. S. Semeikin, I. S. Migalova, S. Wolowiec, *Mendeleev Commun.* **1999**, *9*, 134; c) P. A. Stuzhin, S. S. Ivanova, I. S. Migalova, *Russ. J. Gen. Chem.* **2004**, 74, 1435; d) H. Ogata, T. Fukuda, K. Nakai, Y. Fujimura, S. Neya, P. A. Stuzhin, N. Kobayashi, *Eur. J. Org. Chem.* **2004**, 1621; e) N. Pan, Y. Bian, T. Fukuda, M. Yokoyama, R. Li, S. Neya, J. Jiang, N. Kobayashi, *Inorg. Chem.* **2004**, *43*, 8242; f) H. Shinmori, F. Kodaira, S. Matsugo, S. Kawabata, A. Osuka, *Chem. Lett.* **2005**, *34*, 322; g) Y. Ohgo, S. Neya, H. Uekusa, M. Nakamura, *Chem. Commun.* **2006**, 4590; h) N. E. Galanin, L. A. Yakubov, E. V. Kudrik, G. P. Shaposhnikov, *Russ. J. Gen. Chem.* **2008**, 78, 1436; i) N. Pan, Y. Bian, M. Yokoyama, R. Li, T. Fukuda, S. Neya, J. Jiang, N. Kobayashi, *Eur. J. Inorg. Chem.* **2008**, 5519; j) P. A. Stuzhin, S. E. Nefedov, R. S. Kumeev, A. Ul-Haq, V. V. Minin, S. S. Ivanova, *Inorg. Chem.* **2010**, *49*, 4802; k) T. Okujima, G. Jin, S. Otsubo, S. Aramaki, N. Ono, H. Yamada, H. Uno, *J. Porphyrins Phthalocyanines* **2011**, *15*, 697; l) P. A. Stuzhin, A. Ul-Haq, S. E. Nefedov, R. S. Kumeev, O. I. Koifman, *Eur. J. Inorg. Chem.* **2011**, 2567.

[5] Two β-free DAP–copper complexes including **4Cu** were reported in a patent, although the yields and the spectral data are not described: A. Ogiso, S. Inoue, T. Nishimoto, H. Tsukahara, T. Misawa, T. Koike, N. Mihara, S. Murayama, R. Nara, WO-A1–2001047719, **2001**.

[6] a) R. L. N. Harris, A. W. Johnson, I. T. Kay, *J. Chem. Soc. C* **1966**, 22; b) O. G. Khelevina, N. V. Chizhova, P. A. Stuzhin, A. S. Semeikin, B. D. Berezin, *Russ. J. Coord. Chem.* **1997**, *71*, 74.

[7] Modified porphyrins containing a fused pyridinone unit (oxypyriporphyrins) were reported by a few research groups: a) T. D. Lash, S. T. Chaney, *Chem. Eur. J.* **1996**, *2*, 944; b) T. Schönemeier, E. Breitmaier, *Synthesis* **1997**, 273; c) T. D. Lash, S. T. Chaney, *J. Org. Chem.* **1998**, *63*, 9076; d) H. Eguchi, Y. Ohgo, A. Ikezaki, S. Neya, M. Nakamura, *Chem. Lett.* **2008**, *37*, 768; e) S. Neya, M. Suzuki, H. Ode, T. Hoshino, Y. Furutani, H. Kandori, H. Hori, K. Imai, T. Komatsu, *Inorg. Chem.* **2008**, *47*, 10771.

[8] Shinokubo et al. have independently developed an efficient synthetic procedure for azacorroles by Pd-catalyzed amination of a dichlorodipyrrin complex. M. Horie, Y. Hayashi, S. Yamaguchi, H. Shinokubo, *Chem. Eur. J.* **2012**, DOI: 10.1002/chem.201200485.

[9] a) K. Singh, *Trans. Faraday Soc.* **1959**, *55*, 124; b) Y. Yamamoto, N. Asao, *J. Org. Chem.* **1990**, *55*, 5303.

[10] **CAUTION**! Although we have not experienced it, heavy-metal azides are believed to be explosive in nature. Therefore, care must be taken with CuN_3 in the reaction procedure.

[11] All attempts to convert **4Ni** and **4Cu** to a freebase by treatment with protic acids (CF_3CO_2H, conc. H_2SO_4, conc. H_2SO_4–CF_3CO_2H) have so far failed.

[12] **3Ni**: $C_{36}H_{30}Br_4N_4Ni$, $M_w=896.99\,g\,mol^{-1}$; $0.40\times0.15\times0.05$ mm; monoclinic; $P2_1/n$; $a=10.909(2)$, $b=11.443(3)$, $c=27.564(6)$ Å; $\beta=94.261(3)°$; $V=3431.3(13)$ Å^3; $Z=4$; $\rho_{calcd}=1.736\,g\,cm^{-3}$; $m=52.55\,cm^{-1}$; collected reflections 25914; independent 7665; parameters 406; $R_w=0.1385$, $R=0.0521$ [$I>2.0\sigma(I)$]; GOF=1.094. **3Cu**: $C_{36}H_{30}Br_4CuN_4$; $M_w=901.82\,g\,mol^{-1}$; $0.40\times0.10\times0.03$ mm; triclinic; P-1; $a=11.2953(13)$, $b=12.5757(16)$, $c=26.170(4)$ Å; $\alpha=89.482(5)$, $\beta=78.093(5)$, $\gamma=71.624(4)°$; $V=3445.6(8)$ Å^3; $Z=4$; $\rho_{calcd}=1.738\,g\,cm^{-3}$; $\mu=53.04\,cm^{-1}$; collected reflections 27377; independent 15074; parameters 811; $R_w=0.1238$; $R=0.0521$ [$I>2.0\sigma(I)$]; GOF=1.113. **4Ni**: $C_{36}H_{30}N_6Ni$; $M_w=605.37\,g\,mol^{-1}$; $0.20\times0.10\times0.03$ mm; monoclinic; $P2_1/c$; $a=8.400(2)$, $b=23.910(6)$, $c=7.694(2)$ Å; $\beta=112.673(3)°$; $V=1426.0(6)$ Å^3; $Z=2$; $\rho_{calcd}=1.410\,g\,cm^{-3}$; $\mu=7.18\,cm^{-1}$; collected reflections 11067; independent 3176; parameters 196; $R_w=0.0967$; $R=0.0388$ ($I>2.00\sigma(I)$); GOF=1.071. **4Cu**: $C_{36}H_{30}CuN_6$; $M_w=610.20\,g\,mol^{-1}$; $0.60\times0.25\times0.02$ mm; monoclinic; $P2_1/c$; $a=8.285(4)$, $b=24.560(12)$, $c=7.417(4)$ Å; $\beta=109.722(5)°$; $V=1420.8(12)$ Å^3; $Z=2$; $\rho_{calcd}=1.426\,g\,cm^{-3}$; $\mu=8.07\,cm^{-1}$; collected reflections 10312; independent 3241; parameters 196; $R_w=0.1305$; $R=0.0532$ [$I>2.0\sigma(I)$]; GOF=1.074. **5Ni**: $C_{36}H_{31}N_7Ni$; $M_w=620.39\,g\,mol^{-1}$; $0.20\times0.15\times0.05$ mm; trigonal; $P3$; $a,b=15.508(2)$, $c=10.9418(11)$ Å; $\gamma=120°$; $V=2278.9(5)$ Å^3; $Z=3$; $\rho_{calcd}=1.356\,g\,cm^{-3}$; $\mu=6.77\,cm^{-1}$; collected reflections 10286; independent 4479; parameters 406; $R_w=0.1476$; $R=0.0678$ [$I>2.0\sigma(I)$]; GOF=1.141. **9**: $C_{60}H_{46}N_6Ni$; $M_w=909.74\,g\,mol^{-1}$; $0.30\times0.10\times0.03$ mm; monoclinic; $Pbca$; $a=11.878(2)$, $b=19.174(4)$, $c=19.389(4)$ Å; $V=4416.0(14)$ Å^3; $Z=4$; $\rho_{calcd}=1.368\,g\,cm^{-3}$; $\mu=4.90\,cm^{-1}$; collected reflections 33148; independent 5067; parameters 304; $R_w=0.1421$; $R=0.0690$ [$I>2.0\sigma(I)$]; GOF=1.235. **11**: $C_{36}H_{28}Br_2N_6NiO$; $M_w=779.17\,g\,mol^{-1}$; $0.25\times0.04\times0.03$ mm; monoclinic; $P2_1/c$; $a=8.463(4)$, $b=13.769(7)$, $c=27.102(15)$ Å; $\beta=93.889(9)°$; $V=3151(3)$ Å^3; $Z=4$; $\rho_{calcd}=1.643\,g\,cm^{-3}$; $\mu=31.93\,cm^{-1}$; collected reflections 24083; independent 7158; parameters 415; $R_w=0.2062$; $R=0.0787$ [$I>2.0\sigma(I)$]; GOF=1.159.

[13] H. S. Gill, I. Finger, I. Božidarević, F. Szydlo, M. J. Scott, *New J. Chem.* **2005**, *29*, 68.

[14] Y. Kawamata, S. Tokuji, H. Yorimitsu, A. Osuka, *Angew. Chem.* **2011**, *123*, 9029; *Angew. Chem. Int. Ed.* **2011**, *50*, 8867. λ_{Soret} and λ_Q of **P1** in CH_2Cl_2 were reported to be 424 and 562 nm, respectively.

[15] O. B. Locos, D. P. Arnold, *Org. Biomol. Chem.* **2006**, *4*, 902. λ_{Soret} and λ_Q of **P2** in $CHCl_3$ were reported to be 403 and 546 nm, respectively.

[16] T. Rohand, E. Dolusic, T. H. Ngo, W. Maes, W. Dehaen, *ARKIVOC* **2007**, 307.

[17] a) SIR92 (for **3Ni**, **3Cu**, **4Ni**, **4Cu**, **9**, and **11**): A. Altomare, G. Cascarano, C. Giacovazzo, A. Guagliardi, M. Burla, G. Polidori, M. Camalli, *J. Appl. Crystallogr.* **1994**, *27*, 435; b) SIR2008 (for **5Ni**): M. Burla, R. Caliandro, M. Camalli, B. Carrozzini, G. L. Cascarano, L. De Caro, C. Giacovazzo, G. Polidori, D. Siliqi, R. Spagna *J. Appl. Crystallogr.* **2007**, *40*, 609.

[18] SHELXL-97: G. M. Sheldrick, *Acta Crystallogr.* **1997**, *A64*, 112.

[19] CrystalStructure 4.0: Crystal Structure Analysis Package, Rigaku Corporation (**2000–2010**), Tokyo 196–8666, Japan.

[20] R. Krishnan, J. S. Binkley, R. Seeger, J. A. Pople, *J. Chem. Phys.* **1980**, *72*, 650.

[21] a) A. J. H. Wachters, *J. Chem. Phys.* **1970**, *52*, 1033–1036; b) P. J. Hay, *J. Chem. Phys.* **1977**, *66*, 4377; c) K. Raghavachari, G. W. Trucks, *J. Chem. Phys.* **1989**, *91*, 1062.

[22] a) A. D. Becke, *J. Chem. Phys.* **1993**, *98*, 5648; b) C. Lee, W. Yang, R. G. Parr, *Phys. Rev. B* **1988**, *37*, 785.

[23] Gaussian 09, Revision B.01, M. J. Frisch, G. W. Trucks, H. B. Schlegel, G. E. Scuseria, M. A. Robb, J. R. Cheeseman, G. Scalmani, V. Barone, B. Mennucci, G. A. Petersson, H. Nakatsuji, M. Caricato, X. Li, H. P. Hratchian, A. F. Izmaylov, J. Bloino, G. Zheng, J. L. Sonnenberg, M. Hada, M. Ehara, K. Toyota, R. Fukuda, J. Hasegawa, M. Ishida, T. Nakajima, Y. Honda, O. Kitao, H. Nakai, T. Vreven,

J. A. Montgomery, Jr., J. E. Peralta, F. Ogliaro, M. Bearpark, J. J. Heyd, E. Brothers, K. N. Kudin, V. N. Staroverov, R. Kobayashi, J. Normand, K. Raghavachari, A. Rendell, J. C. Burant, S. S. Iyengar, J. Tomasi, M. Cossi, N. Rega, J. M. Millam, M. Klene, J. E. Knox, J. B. Cross, V. Bakken, C. Adamo, J. Jaramillo, R. Gomperts, R. E. Stratmann, O. Yazyev, A. J. Austin, R. Cammi, C. Pomelli, J. W. Ochterski, R. L. Martin, K. Morokuma, V. G. Zakrzewski, G. A. Voth, P. Salvador, J. J. Dannenberg, S. Dapprich, A. D. Daniels, Ö. Farkas, J. B. Foresman, J. V. Ortiz, J. Cioslowski, D. J. Fox, Gaussian, Inc., Wallingford CT, **2009**.

Received: February 13, 2012
Published online: March 30, 2012

